

## Isolation and Characterization of a Previously Undetected Human cAMP Phosphodiesterase by Complementation of cAMP Phosphodiesterase-deficient *Saccharomyces cerevisiae*\*

(Received for publication, October 1, 1992, and in revised form, March 1, 1993)

Tamar Michaeli†§, Tim J. Bloom¶, Tim Martins||, Kate Loughney||, Ken Ferguson||, Michael Riggs, Linda Rodgers, Joseph A. Beavo¶, and Michael Wigler‡\*\*

From the ‡Cold Spring Harbor Laboratory, Cold Spring Harbor, New York 11724, the ||ICOS Corporation, Bothell, Washington 98021, and the ¶Department of Pharmacology, University of Washington, Seattle, Washington 98195

We have established a highly sensitive functional screen for the isolation of cDNAs encoding cAMP phosphodiesterases (PDEs) by complementation of defects in a *Saccharomyces cerevisiae* strain lacking both endogenous cAMP PDE genes, *PDE1* and *PDE2*. Three groups of cDNAs corresponding to three distinct human genes encoding cAMP-specific PDEs were isolated from a human glioblastoma cDNA library using this functional screen. Two of these genes are closely related to the *Drosophila dunce* cAMP-specific PDE. The third gene, which we named *HCP1*, encoded a novel cAMP-specific PDE. *HCP1* has an amino acid sequence related to the sequences of the catalytic domains of all cyclic nucleotide PDEs. *HCP1* is a high affinity cAMP-specific PDE ( $K_m = 0.2 \mu\text{M}$ ) that does not share other properties of the cAMP-specific PDE family, i.e. extensive sequence homology to the *Drosophila dunce* cAMP PDE and sensitivity to rolipram and R020-1724. The PDE activity of *HCP1* is not sensitive to cGMP or other inhibitors of the cGMP-inhibitable PDEs, such as milrinone. The biochemical and pharmacological properties of *HCP1* suggest that it is a member of a previously undiscovered cyclic nucleotide PDE family. Northern blot analysis indicates that high levels of *HCP1* mRNA are present in human skeletal muscle.

Cyclic nucleotides serve as second messengers that mediate a variety of cellular responses to extracellular signals such as hormones, light, and neurotransmitters. Cyclic nucleotide phosphodiesterases (PDEs)<sup>1</sup> play a role in signal transduction by regulating the cellular concentrations of cyclic nucleotides (reviewed in Ref. 1). Mammalian cells contain multiple PDEs that have been distinguished into six families based on their substrate affinity and specificity and on their selective sensi-

tivity to cofactors and inhibitory drugs (reviewed in Refs. 2 and 3). These families are (I) Ca<sup>2+</sup>/calmodulin-dependent PDEs, (II) cGMP-stimulated PDEs, (III) cGMP-inhibited PDEs, (IV) cAMP-specific PDEs, (V) cGMP-specific PDEs, and (VI) photoreceptor PDEs. As the amino acid sequences of members of these PDE families are being determined, it is becoming apparent that all these PDE families contain a related domain, thought to be the catalytic domain, with ~30% sequence identity between families (2). Members of the same family are more closely related, and the available sequences suggest that they share between 60–80% sequence identity extending throughout the entire coding region (2, 4).

Two PDE genes, *PDE1* and *PDE2*, have been identified and cloned from the yeast, *Saccharomyces cerevisiae* (5–8). *PDE2* is a high affinity cAMP-specific PDE related in sequence to PDEs of mammalian cells. *PDE1* is a low affinity cAMP-specific PDE that belongs to a different evolutionary branch of PDEs. The *PDE1* sequence is more closely related to the secreted PDE form of *Dictyostelium discoideum* than to *PDE2* and the known mammalian cell PDEs.

In *S. cerevisiae*, RAS proteins are regulators of adenylyl cyclase and of cAMP production (9). The mutationally activated *RAS2* gene, *RAS2*<sup>val19</sup>, leads to an increase of cellular cAMP content and to several associated phenotypes (9–11). Among the phenotypes that result from expression of *RAS2*<sup>val19</sup> is an acute sensitivity to heat shock. The yeast *PDE1* and *PDE2* genes were isolated as multicopy suppressors of the *RAS2*<sup>val19</sup> heat shock phenotype. In a similar manner, two mammalian cDNAs encoding cAMP-specific PDEs were previously isolated: rat (*DPD*) and human (*JC44*) cDNAs, both encoding homologs of the *Drosophila dunce* cAMP PDE and members of family IV (12, 13). In this study we describe the establishment of a more sensitive functional screen for isolation of cDNAs encoding cAMP PDEs and its use to isolate a human cDNA that appears to define a new family of PDE genes.

### EXPERIMENTAL PROCEDURES

**Strains, Growth Conditions, Heat Shock Assays, and Segregation Analysis**—Plasmids were propagated in *Escherichia coli* strains HB101 or SCS1 (Stratagene). *S. cerevisiae* strains *TK161-R2V*: (*MATa RAS2*<sup>val19</sup> *leu2 his3 ura3 ade8 trp1*) (9) and *10DAB* (*MATa leu2 his3 ura3 ade8 pde1::ADE8 pde2::URA3 ras1::HIS3*) (12) were grown in rich medium (YPD) or synthetic medium (SC) with appropriate supplements. Heat shock assays of variable time periods were performed as previously described (12). To screen the expression library, yeast transformants were plated at approximately 10<sup>3</sup> colonies/plate on selective medium. Colonies were allowed to grow for 3 days and then replica plated onto preheated plates. Heat shocks were carried out at 55 °C for 15 min and followed by 2–3 days of recovery at 30 °C. Surviving colonies were picked, restreaked on synthetic

\* This work was supported by the National Cancer Institute, the American Cancer Society, and National Institutes of Health. The costs of publication of this article were defrayed in part by the payment of page charges. This article must therefore be hereby marked "advertisement" in accordance with 18 U.S.C. Section 1734 solely to indicate this fact.

The nucleotide sequence(s) reported in this paper has been submitted to the GenBank™/EMBL Data Bank with accession number(s) L12052.

§ Present address: Dept. Devel. Biol. & Cancer, Albert Einstein College of Medicine, 1300 Morris Park Ave., Bronx, NY 10461.

\*\* American Cancer Society Research Professor. To whom correspondence should be addressed: Cold Spring Harbor Lab., P. O. Box 100, Cold Spring Harbor, NY 11724. Tel.: 516-367-8376; Fax: 516-367-8381.

<sup>1</sup> The abbreviations used are: PDEs, phosphodiesterases; kb, kilobase(s); PCR, polymerase chain reaction; ORF, open reading frame.

medium plates for colony purification, and then cultured in rich medium for 2–3 days to allow for plasmid loss from some cells.  $10^{-6}$  ml of these cultures were then plated onto YPD plates. After 2–3 days of growth, these plates were replica plated onto synthetic medium plates (Leu<sup>+</sup> selection), YPD plates, and YPD heat shock plates. Colonies were scored to ascertain if the observed heat shock resistance was plasmid-dependent.

**Plasmid, DNA Manipulations, and Sequencing**—The plasmids employed in this study are expression vectors containing the ADH1 promoter, the yeast 2 $\mu$  replication origin, and the LEU2 selectable marker: ADNS was described previously (12) and AD54 is a derivative of ADNS in which the ADH1 promoter is attached to an epitope derived from the influenza hemagglutinin protein. The DNA sequence encoding this epitope tag ends with a *Sa*I restriction endonuclease site and is followed by the portion of the pUC18 polylinker residing between the *Sa*I and the *Eco*R I sites. TM22 $\Delta$  was generated by deleting the 0.5-kb *Bgl*II fragment of TM22. L22M1 through 4 were generated by inserting PCR-amplified DNA fragments of TM22, which were flanked by *Sa*I sites, into the *Sa*I site of AD54. The 20-cycle PCR amplification was performed under standard conditions. PCR reactions for generating the *Sa*I fragments of L22M1–4 included a common COOH-terminal oligonucleotide 5'-GCTAGTTCGACCTGGCTGGCATCACTCAC (1603). The NH<sub>2</sub>-terminal oligonucleotides included in these PCR reactions were: L22M1, 5'-GCTAGTCGACGATGGAAGTGTGTACCAG (68); L22M2, 5'-CGTAGTCGACTATGCTAGGAGATGTACGTG (261); L22M3, 5'-CGTAGTCGACCATGCTGGAAAAAGTTGGA (506); L22M4, 5'-CGTAGTCGACCATGATGAAACTTCGTAGA (638). The numbers indicate the coordinates, as in Fig. 2. The DNA sequence of the PCR-generated *Sa*I fragment of L22M4 was determined and found to be identical to the corresponding TM22 sequence.

Sequencing was performed by the dideoxynucleotide chain-termination method (14, 15). Both strands of the TM22 4.0-kb *Not*I fragment were sequenced as detailed in the strategy shown in Fig. 2.

**Northern Blotting**—Cytoplasmic RNA from the U118-MG cell line was isolated in a buffer containing 140 mM NaCl, 1.5 mM MgCl<sub>2</sub>, 10 mM Tris-Cl, pH 8.6, and 0.5% Nonidet P-40. Following a 1.5-min 12,000  $\times$  g spin, the supernatant was incubated with 0.5 mg/ml proteinase K for 30 min at room temperature, extracted with a 1:1 phenol/chloroform mixture, and ethanol precipitated. Poly(A)<sup>+</sup> RNA was selected on oligo(dT) by established procedures (16). RNA was fractionated on a 1% formaldehyde-agarose gel and transferred onto a nylon membrane (GeneScreen Plus, New England Nuclear). The membrane was baked at 80 °C for 2 h. Hybridization was performed at 60 °C in 1% sodium dodecyl sulfate, 1 M sodium chloride, and 10% dextran sulfate. Following hybridization the membrane was washed at 60 °C in 0.3 M sodium chloride, 0.03 M sodium citrate, and 1% sodium dodecyl sulfate. The membrane was stripped of the radioactive probe by a 10-minute incubation in boiling water. Removal of the radioactivity from the membrane was monitored by autoradiography. RNA probe complementary to ORF2 was transcribed *in vitro* by T7 RNA polymerase from a template containing the *Spe*I-*Nsi*I fragment (base pair 3372–3646) of TM22 (Fig. 2). Hybridization of this [<sup>32</sup>P]CTP-labeled probe was performed at 42 °C in the hybridization buffer described, except with the addition of 50% formamide. Washes were performed as detailed above.

Blots of size-fractionated poly(A)<sup>+</sup> RNA from human tissues were purchased from Clontech, Inc. Blots were hybridized to <sup>32</sup>P-labeled DNA probes at 43 °C in 50% formamide, 0.75 M sodium chloride, 50 mM sodium phosphate monobasic, pH 7.4, 50 mM EDTA, 0.16% Ficoll, 0.16% polyvinylpyrrolidone, 0.16% bovine serum albumin, 0.18% sodium dodecyl sulfate, and 100  $\mu$ g/ml denatured salmon sperm DNA. Following hybridization the blots were washed under stringent conditions for 20 min at 50 and at 65 °C in 0.015 M sodium chloride, 0.0015 M sodium citrate (0.1  $\times$  SSC), and 0.5% sodium dodecyl sulfate. One blot was first hybridized to a 650-nucleotide long single-stranded DNA probe, generated by PCR, complementary to the 5' end of TM22, and then to the nick-translated double-stranded probe (1.2-kb *Not*I-*Eco*RI fragment of TM22). The hybridization pattern of the single-stranded probe was identical to the double-stranded HCP1 probe (not shown).

**Phosphodiesterase Assays**—Yeast cells were grown at 30 °C in synthetic medium (SC-leucine). Cells were harvested and resuspended in lysis buffer containing 50 mM potassium phosphate, pH 7.4, 150 mM NaCl, and 30 mM benzimidazole. Cells were broken with glass beads, and cellular debris was removed by a 5-min spin at 12,000  $\times$  g.

Cyclic nucleotide phosphodiesterase activity in the supernatant

was measured as previously described, with modifications (17, 18). Assays were performed in vinyl microtiter plates (Costar) at 30 °C. Incubation mixtures contained 40 mM Tris-Cl, pH 8.0, 1 mM EGTA, 5 mM magnesium chloride, 0.1 mg/ml bovine serum albumin, diluted enzyme, [<sup>3</sup>H]cyclic nucleotides (0.14  $\mu$ Ci/assay) (New England Nuclear), [<sup>14</sup>C]AMP (0.01  $\mu$ Ci/assay) (New England Nuclear), and varying amounts of unlabeled cyclic nucleotides in a total volume of 125  $\mu$ l. The assays were terminated by removing a 100- $\mu$ l aliquot of the reaction mixture to a microliter well containing 100  $\mu$ l of stop buffer (0.2 M ethanolamine, pH 9.0, 1 M ammonium sulfate, 20 mM EDTA, and 1% SDS). The 5' nucleotide products were separated from the unreacted cyclic nucleotides by chromatography on columns (8  $\times$  5 mm) containing Affi-Gel 601 (Bio-Rad), an acrylamide matrix containing covalently coupled aminophenylboronate. The columns were washed with 2.5 ml of wash buffer containing 0.1 M ethanolamine, pH 9.0, and 0.5 M ammonium sulfate. The columns were then eluted with 2 ml of elution buffer containing 0.25 M acetic acid. The column eluate that collected into the vials was mixed with scintillation fluid (EcoLume, ICN Biochemicals) and analyzed for <sup>3</sup>H and <sup>14</sup>C content by dual channel liquid scintillation spectroscopy. The recovery of <sup>3</sup>H nucleotide reaction products were corrected for the recovery of [<sup>14</sup>C]AMP. All the kinetic data points represent measurements of initial rates, determined by incubations for multiple intervals at suitable enzyme dilutions. One unit of phosphodiesterase activity is expressed as 1  $\mu$ mol of cyclic nucleotide hydrolyzed/min  $\cdot$  mg protein.

## RESULTS

**Isolation of Human cDNAs Encoding cAMP PDEs**—Several mammalian homologs of the *Drosophila* dunce cAMP PDE have been previously isolated from cDNA expression libraries based on their ability to suppress the heat shock-sensitive phenotype of *RAS2*<sup>val19</sup> (12, 13). In this study we identified two new human genes encoding cAMP PDEs. cDNAs corresponding to these genes were isolated based on their ability to suppress the heat shock-sensitive phenotype of the strain 10DAB, a strain in which the two yeast cAMP PDE genes have been disrupted.

The strain 10DAB was transformed with a yeast expression library containing cDNAs derived from the human glioblastoma cell line U118-MG (Human Tumor Cell Line Bank, Human Tumor Cell Laboratory, Memorial Sloan-Kettering Cancer Institute, 13). 10<sup>5</sup> transformants were screened for their ability to withstand heat shock at 55 °C by the replica plate method. Seventy-four colonies were found to contain plasmids capable of rendering 10DAB cells resistant to heat shock. These plasmids contained three groups of cDNAs. The largest group, with 70 members, contained cDNAs that were variants of JC44 and of the previously isolated high affinity rolipram-sensitive cAMP-specific PDE (13, 19). The second group, represented by TM72, contained two cDNA clones encoding an additional member of the high affinity, rolipram-sensitive, cAMP-specific PDE family that will be described elsewhere.<sup>2</sup> The amino acid sequence of these two groups are highly related to the *D. melanogaster* dunce cAMP PDE and to the four dunce homologs found in rat (12, 13, 19–21).

The third group, represented by TM22, contained two cDNA clones encoding a novel PDE whose properties are detailed in this study. The ability of TM22 to render 10DAB cells resistant to heat shock is depicted in Fig. 1.

Representative cDNAs from all three groups that were isolated as suppressors of deficiencies in cAMP PDEs of the strain 10DAB failed to suppress the heat shock sensitivity of *RAS2*<sup>val19</sup> (Fig. 1).<sup>3</sup> However, JC44, a structural variant of cAMP-specific PDEs of the first group has been isolated as a

<sup>2</sup> G. Bolger, T. Michaeli, T. Martins, T. St. John, B. Steiner, L. Rodgers, M. Riggs, M. Wigler, and K. Ferguson, manuscript in preparation.

<sup>3</sup> T. Michaeli, T. Bloom, T. Martins, K. Loughney, K. Ferguson, M. Riggs, L. Rodgers, J. Beavo, and M. Wigler, unpublished observations.

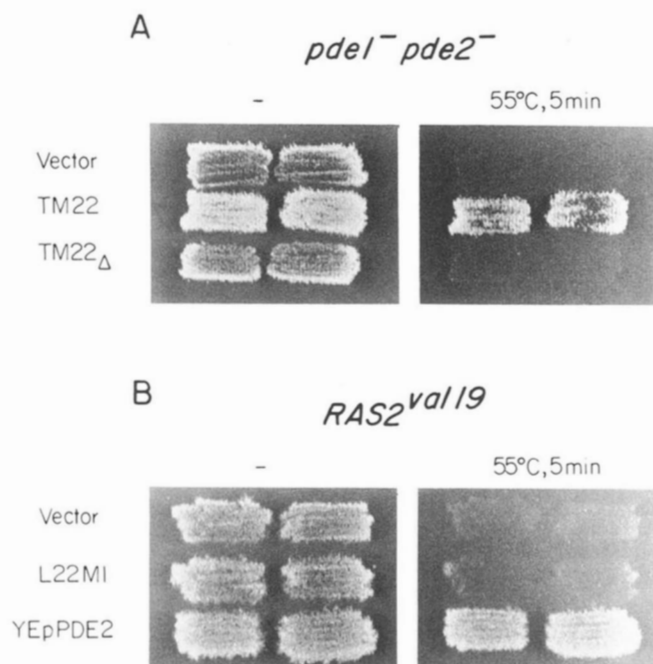


**FIG. 1. Suppression of the *pde1<sup>-</sup>pde2<sup>-</sup>* and the *RAS2<sup>val19</sup>* heat shock phenotypes.** A, 10DAB cells were transformed with the ADNS vector, with TM22, and with a deletion mutant of TM22, TM22 $\Delta$ . B, *RAS2<sup>val19</sup>* cells were transformed with the AD54 vector, with L22M1, an expression vector of the TM22 cDNA, and with YEpPDE2, a plasmid containing the yeast PDE2 gene. Two independent transformants were patched onto SC-leucine plates, grown at 30 °C for 3 days and then replica plated onto a control plate and onto an experimental plate that was subjected to a 5-min heat shock treatment at 55 °C. Plates were photographed following a 24-h recovery period at 30 °C. See also Fig. 5.

suppressor of *RAS2<sup>val19</sup>* (13). Thus, it appears that *pde1<sup>-</sup>pde2<sup>-</sup>* cells are more sensitive to the effects of cAMP phosphodiesterases than are *RAS2<sup>val19</sup>* cells.

**Sequence of TM22**—The cDNA insert of TM22 was a 4.0-kb DNA fragment flanked by the restriction sites of the *NotI* endonuclease used in its cloning (13). The DNA sequence of this fragment revealed two open reading frames (Fig. 2). The first open reading frame, called ORF1, was 498 amino acids long with the first ATG appearing at codon 17. The termination codon of this open reading frame was followed by a 2.5-kb non-coding DNA fragment ending with a *NotI* restriction endonuclease cleavage site. An additional open reading frame of 293 amino acids, named ORF2, was found on the non-coding strand on the distal 1.0 kb end of the cDNA (between nucleotides 3048–3817). The initiator methionine of ORF2 was preceded by a termination codon. To determine which of the two open reading frames played a role in suppressing *pde1<sup>-</sup>pde2<sup>-</sup>* defects, we generated an in-frame deletion in ORF1, TM22 $\Delta$ . This deletion mutant failed to suppress the heat shock sensitivity of 10DAB (Fig. 1). Thus, ORF1 is required for suppression of *pde1<sup>-</sup>pde2<sup>-</sup>* defects. The gene corresponding to ORF1 was subsequently named *HCP1*, for reasons discussed later.

Additional cDNAs isolated from a second cDNA library derived from the U118-MG cell line and from a human heart cDNA library by screening with DNA probes encompassing ORF1 were characterized by sequencing. The structure of these cDNAs indicated that inefficient polyadenylation may account for the formation of a read-through transcript with the structure of the TM22 cDNA. One group of cDNAs included several members that, like TM22, contained parts of ORF1, lacked a poly(A) tail, and extended to various extents

into the COOH terminus of ORF2. The structure of this group of cDNAs suggests that TM22 is not an aberrant fusion product generated by reverse transcriptase. A second group of cDNAs included several members that contained parts of ORF1 and were polyadenylated at either of two adjacent locations, following nucleotides 3104 and 3106. A polyadenylation AATAAA consensus sequence was found 15–17 nucleotides upstream of these sites, and they are followed by a T-rich region (reviewed in Ref. 22). This putative polyadenylation site lies within ORF2. The structure of these cDNAs suggests that the two open reading frames might be normally found on two independent transcripts.

To confirm the relationships between the two open reading frames and the structure of the isolated cDNA insert, we have tested whether the two open reading frames were indeed found on two independent transcripts. For this purpose we performed a Northern blot analysis of poly(A)<sup>+</sup> RNA from U118-MG cells (Fig. 3). The blot was first hybridized to a 1.2-kb *NotI-EcoRI* DNA fragment that contained most of ORF1 and none of the sequences downstream of it. This DNA probe hybridized to a single mRNA band estimated to be 4.5 kb in size. The blot was stripped of this probe, and hybridized to a 1.0-kb *BstXI-NotI* DNA fragment encompassing ORF2 and about 50 base pairs of the non-coding sequence downstream of its COOH terminus. This probe hybridized strongly to a 6.0-kb mRNA band and very weakly to the same size band to which ORF1 hybridized (~4.5 kb). A single-stranded RNA probe containing sequences complementary to ORF2 hybridized to a 6.0-kb mRNA band as well (data not shown). The weak hybridization of the double-stranded ORF2 probe to the 4.5-kb ORF1 mRNA band is probably due to the fact that it contained about 110 base pairs upstream of the putative poly(A) site of ORF1 (HCP1). Thus, the two open reading frames are found on two independent transcripts.

The location of the polyadenylation sites and the size of the HCP1 mRNA might indicate that TM22 is a partial cDNA clone of HCP1 which contains only 3 kb of the 4.5-kb mRNA detected on Northern blots. It is therefore not clear whether the first ATG found in ORF1 serves as the initiator methionine of HCP1. Attempts to isolate additional 5' sequences of the HCP1 mRNA have met with persistent obstacles. We additionally screened three cDNA libraries derived from human brain, two from heart, and a second from the U118-MG cell line. Each library screen yielded HCP1 cDNA clones, but their DNA sequence indicated that none extended 5' of the known TM22 sequences. The difficulties in obtaining full-length clones may be due, in part, to the high GC content (82%) of the 5' end of TM22, or may reflect that the 5' sequences already cloned represent the 5' end of the transcript.

**Similarities between HCP1 and cAMP PDEs**—A search for sequences similar to HCP1 in the data banks revealed a strong homology to cAMP PDEs. The alignment of a portion of HCP1 to representative members of several cAMP PDE families whose sequences are known is shown in Fig. 4. Represented were the cAMP-specific PDEs (rat DPD), the Ca<sup>2+</sup>/calmodulin-dependent cyclic nucleotide PDEs (61-kDa bovine brain form) and the bovine cGMP-stimulated PDE (4, 12, 23). Significant homology was observed in a COOH-terminal region of ~300 amino acids, thought to constitute the catalytic portion of these enzymes (24–28). The homology encompassed the region between residues 164–451 of HCP1. Sequence relatedness among these PDEs was determined by the MACAW program (29) which defined within this COOH-terminal region seven homology blocks (A–G), interspersed by short unrelated sequences.

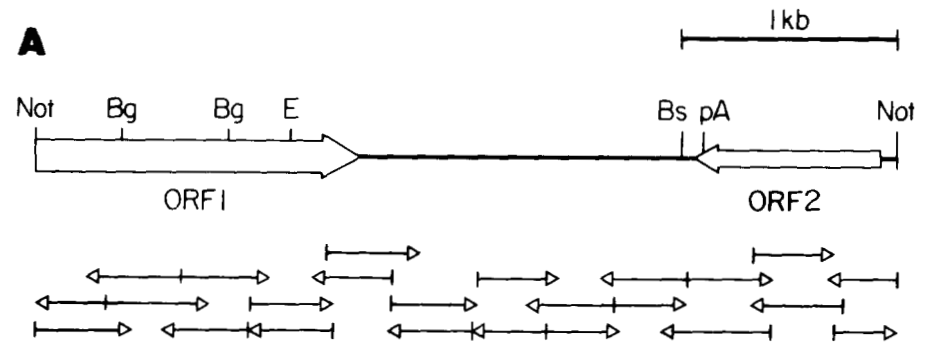


**FIG. 2. Structure and sequences of TM22.** *A*, a diagram of the structure of the TM22 cDNA includes the location and direction of the two open reading frames, ORF1 and ORF2, marked by arrows. The location of the polyadenylation sites of ORF1 is marked by pA. The location of the restriction endonuclease cleavage sites *Bgl*II (*Bg*), *Bst*XI (*Bs*), *Eco*RI (*E*), and *Not*I (*Not*) are indicated. The sequencing strategy of TM22 is detailed below the diagram: the orientation and length of the fragments sequenced with a single oligonucleotide are detailed. *B*, the DNA sequence of TM22 and the predicted amino acid sequence of ORF1 are presented. Coordinates on the right indicate nucleotide and amino acid positions. The polyadenylation sites of ORF1 (nucleotides 3104 and 3106) are underlined and in **bold type**, and upstream of these sites is the polyadenylation consensus sequence AATAAA (underlined). The location of sequences used to generate L22M1-4 is indicated by the arrows labeled M1-M4, respectively.

**B**

```

CGCGCCCGCCGAGCCGCGCCGCGGAGCCGCGCGGCGTATCAATGGAAGTGTCTTACCAGCTGGCGTACTGCCCTGGACGGCCGGTCCCGCAGCAGCTCCTCAGCCGCGGA 122
ArgProArgClnGlyGlyArgArgAlaGluAlaGlyArgAlaTyrSerMETGluValCysTyrGlnLeuProValLeuProLeuAspArgProValProGlnHisValLeuSerArgArg 40
M1→
GGAGCCATCAGCTCAGCTCCAGCTCCGCTCTCTCGGCTGCCCAATCCCGCCAGCTCTCTCAGAGGGCTGGAGCTATTCTCATGACAGTCTGATCAGCACTGCATTACATTCGT 242
GlyAlaIleSerPheSerSerSerAlaLeuPheGlyCysProAsnProArgGlnLeuSerGlnArgArgGlyAlaIleSerTyrAspSerSerAspGlnThrAlaLeuTyrIleArg 80
M2→
ATGCTAGGAGTGACTGCTAAGGAGCCGAGCAGGATTTGAATCAGAAAGAGAGGTTCTCACCATATATTGATTTTCGATTTCCACTCTCAATCGAAATGAAGTCTGCTCTCT 362
METLeuGlyAspValArgValArgSerArgAlaGlyPheGluSerGluArgGlySerHisProTyrIleAspPheArgIlePheHisSerGlnSerGluIleGluValSerValSer 120
M3→
GCAAGGAATATCAGAAGGCTACTAAGTTCACGAGATATCTAGATCTCCAGCTTTTTCTGCTGACTCGGTTCAAATTCCTAAACATTTAGATGATGATATAATGGACAGCC 482
AlaArgAsnIleArgArgLeuSerPheGlnArgTyrLeuArgSerSerArgPheArgGlyThrAlaValSerAsnSerLeuAsnIleLeuAspAspAspTyrAsnGlnAla 160
M4→
AAGTGTGCTGGAAAAGTGGAAATTTGATCTTTCTATTGATAGACTAAACAAATAGCTAGTAGCTTAACCTTTTATTTAGTCTTCTGATGATTAAT 602
LysCysMETLeuGluLysValGlyAsnTrpAsnPheAspIlePheLeuPheAspArgLeuThrAsnGlyAsnSerLeuValSerLeuThrPheHisLeuPheSerLeuHisGlyLeuIle 200
CGACTCTCCATTAGATGATGAACTTCGTAGCTTTTGTATGATGATTCAGAAAGATTACACAGCTCAAATCTTACATAAGCAGCTCCAGCTGGGATGTTACTCAGCCAGCT 722
GluTyrPheHisLeuAspMETMETLeuArgArgPheLeuValMETIleGlnGluAspTyrHisSerGlnAsnProTyrHisAsnAlaValHisAlaAlaAspValThrGlnAlaMET 240
CAGTGTACTTAAAGGACCTAAGCTTCCCAATCTGTAAGTCTCTGGGATATCTGCTGAGCTTAATGGAGCTGCCACTCATGATGATCATGAGCTGTTAATCAACCTTCTCT 842
HisCysTyrLeuLysGluProLysLeuAlaAsnSerValThrProTrpAspIleLeuLeuSerLeuIleAlaAlaThrHisAspLeuAspHisProGlyValAsnGlnProPheLeu 280
ATTAACAATCAACTACTTGGCACTTATACAGAATACCTCACTAGCGAAAATCACCAGTGGAGTCTGCGAGTGGCTTATGAGAGAAATCAGGCTTATCTCACATGGCCATTA 962
IleLysThrAsnHisTyrLeuAlaThrLeuTyrLysAsnThrSerValIleGluLysAsnHisHisTrpArgSerAlaValGlyLeuLeuArgGluSerGlyLeuPheSerHisLeuProLeu 320
GAAAGCAGGCAACAATGGAGACAGATAGTGGCTCTGATACAGCCAGACAGTCACTGCCAGAAAGTCAAGTATCTGCTTCTTGGTCCCATTTGGATAGAGGCTGATTTATGCCATA 1082
GluAspThrArgHisArgHisLeuValLeuGlnMETAlaLeuLysCysAlaAspIleCysAsnProCysArgThrTrpGluLeuSerLysGlnTrpSerGluLysValThrGluGluPhe 360
GAAGACACAGACAGACATTTGGTTTACAGATGGCTTTGAAATGCTGATATTTGTAACCCATGCTGGACCTGGGAATTAAGCAGCAGTGGAGTCAAAAAGTCAAGCGAAATTC 1202
GAAAGCAGCAGACAGACATTTGGTTTACAGATGGCTTTGAAATGCTGATATTTGTAACCCATGCTGGACCTGGGAATTAAGCAGCAGTGGAGTCAAAAAGTCAAGCGAAATTC 400
TTCATCAAGGAGATATAGAAAAAATATCATTTGGGTGGAGTCCACTTTCGATGCTCACAGTAACTATGCGCAACATCCAGATTTGGTTTATGATCTACAGTGGAGCTTTA 1322
PheHisGlnGlyAspIleGlyLysTyrHisLeuGlyValSerProLeuCysAspArgHisThrGluSerIleAlaAsnIleGlnIleGlyPheMETThrTyrLeuValGluProLeu 440
TTTACAGAAATGGCCAGGTTTCCCAATACAGGCTATCCCAAGACATGCTGGACAGCTGGGCTGAATAAGCCAGCTGGAGGGAGTGCAGAGAAACAGTGGAGCTGAGGAGCACT 1442
PheThrGluTrpAlaArgPheSerAsnThrArgLeuSerGlnThrMETLeuGlyHisValGlyLeuAsnLysAlaSerTrpLysGlyLeuGlnArgGluGlnSerSerSerGluAspThr 480
GATGCTGCATTTGAGTTCAGCTCACAGTATTACTCTCAGGAAATCGGTTATCATTAACCCCAAGCAGTGGGACAAACTCCCTCTGGAGGTTTTCAGAAATGTAATGGGCTCTG 1562
AspAlaAlaPheGlnLeuAsnSerGlnLeuLeuProGlnGluAsnArgLeuSer . 498
AGGTGAGAGAACTTAAGTCTGACTGCCAAGGTTTCCAACTGAGTGTGCCAGCCAGCATTTTATTTCCAAGATTTCCCTCTGTGGATCATTGAAACCCTTGTAAATTCAGCAAG 1682
CGAACATACAGCAATATGAATTTGGCTTCTCATGTGAACTTGAATATNAAAGCCCGCAGGAGAGAAATCCGAAAGGAGTAAACAAGGAAGTTTGTATATGGCCAGCACTTTTCCAAA 1802
GCATCTAATCTTCAAAACGCTCAACTTGAATTTGTCAGCAACAATCTCTGGAAATTAACCACTGATGCAACAATGTGATCTTGTACTTCCACTAAGTCTCTCTGAGAAAATGGA 1922
AATGTGAAGTGGCCGCTCTGCNTGCCCTGGCAAGCAATGTTTCAAAAATCAACTCTGAAAATATGGTTCTAAATTTGCCCTGGAGCATGATTTGGAAGAACCACTCAACAAATTT 2042
AAAGATCAAACTTACAGCTCTTCCCTGGTTTGGCTTTTCTCTTGGATGCCCAAGGCTCCCATTTGCTATAGTTTATTTCACTGACCTGGAAAGCTGAGCATTTATC 2162
GTAGACTACGCCAAGCTTCCACTCAGTGGCTTGGCAATGCAATTTTATGAGCAATAGTTTATTTAATTTGGGGTGGAGGGGAAACACCAAGTCCCTAGCTGATATGATGCTCT 2282
GCATCAAGACATGCAATGTTTTCACACTGCTACACTGACCTGCACATGGGAGAAAAGTGGAAATGTTTAAACACCAATTAACAGCTCAGNATTTGCCAATCGAAATAAAAG 2402
TGGGATGGGAGAGCGTGTCTTCAGATCAAGGCTACTAAAGTCCCTTTGCTGCGAGTGAAGGATGTTGTGTGGAATGACGGATGTGTGTGNGTGNATGTTTGTGCAATGTA 2522
TGACNGTGCATGATGTTTCTCATGTTGGCCAAAGATTTGAAANGTAGCTTTTATTTATTTAAGAAATGACATAATGAGCAGCAGCACTCGGGGAGGGGAAAGTGGTGGATGTA 2642
AGCTGTAAACAGATTCGCTCAGTGGCTTAACTATGACATAGCTAAGTGACCAAGCTTCTGTTTGAATTTGAAAAGAGTCAATTTTCTTGGCTCCCTTTGATGAAAGCTTACC 2762
CTTTGACGGGCTTTTGTATGAAAGATGTTTCTAGGCAAACTATAAGGCAATTTTAACTTCAAACTTCCACTTTGTAATTTGTTTAAATGTTTATGATAGTAAGCAC 2882
AAGTGTAACTAGTTTAAAGAAACCGGTGCTTTCTTTAGTTCATTTGATTTTCCCTGTTACTGTAAGAGCTGTTTATTAATGTTTACAGTTTGTGCAAGCAGCTATTTCTTGG 3002
GAGAAAGCTGAGTGTAAAGCAATTTGTAAAGGCTTGGCATACTCATTTAAATATGCGCTGTGCTGTTAACTTTGATGATGATAAAACCTATCTTTCAGAAACCTCTCATATA 3122
CAAAATGAAATACATAAGTCTTCTGCTCTCTCAAACCAAACTCTGCAAAATCATAGACAAAGTAAAGCAAACTGATGAAAGTGTTCGATTTGTTGATACCAAGAAACAGGTT 3242
ATAGAGTGAACCTCAAAGCTTCACTCTCAGTAACTATAAGCAATCTCTGTAAGTGTGTAACATAATGCAATGAAGTAACTAACTTTGGATGATTTGAACGGGAAAGAAATCTG 3362
ATGAGCTTCACTGTAATTTCACTGAAATACACAAAGTGTATTAACCAAGTATGCCATGCCCTGAACTGCTGTTGGGATCATCACTGAAACCAATTCAGCCCACTGCTT 3482
GGAGATCTAGGCTTAACTTCTCGTGGCATAGAAATCCAAGCTTCACTGAGTACTCTTCACTGCTGAGGTTATCAGAACTATGCGGCTTTCCCTCACTATCTCATACCCAA 3602
ATACAGCTGTTTAAACAGTATTCTGGCTAAGCAGATCTCATGATATTTAAACTGGCATCTTCCAGGCTAAATATTTCTTCTTCAATATATCTACATATTTGTGTCAC 3722
TGAACAACTGTGCTGCTTCTGTAACCTTCACTTATCTTGGAGTATGCAAGGAAATTTCTATCTGTGTGCTTTGTGCACTACATAGGATCAAAATTCGCTGCAATTC 3842
ACACTTCCCACTCTGCTGTAATAGCAATTTCACTCAAAATCGAAAAGTGGCCATAGAAAGTCCCAAGAAATAAACAATTTTTTTCTCAGCAGGAGCGGAAGCACTAGGG 3962
GGAGCAGGAGCTGCAATGGCCCGC
    
```

The NH<sub>2</sub>-terminal border of this conserved domain was found to extend 40 residues upstream of the boundary previously thought to demarcate homology among the PDEs (2). The extended NH<sub>2</sub>-terminal portion contained homology block A, a poorly conserved spacer, and the first 14 residues of homology block B (Fig. 4, A and B). The sequences of the cGMP-stimulated PDE depicted in homology block A were located 450 residues upstream of block B. However, an additional sequence (A') of the cGMP-stimulated PDE with reduced similarity to sequences of block A was located just upstream of block B of this PDE (Fig. 4C). Although the sequence similarity within homology block A' is poor, its proximity to block B might be of functional importance. An additional structural element of HCP1, an 18-residue NH<sub>2</sub>-

terminal repeat sequence, was found by a double diagonal analysis (Fig. 4D). Within the highly conserved region there were several motifs that were identical among all the known mammalian PDE families and may constitute important structural elements. HCP1 exhibited the highest degree of homology to the cAMP-specific PDE (35% identity, 51% similarity), and the lowest to the cGMP-stimulated PDE (24% identity, 37% similarity). The homology within this region between members of the known cAMP-specific PDE family (family IV), varies between 85-95%, and is not limited to the region depicted in Fig. 4, but extends throughout most of the coding region (data not shown). Thus, it appears that HCP1 is a novel PDE that is more closely related to the cAMP-specific PDEs of family IV,

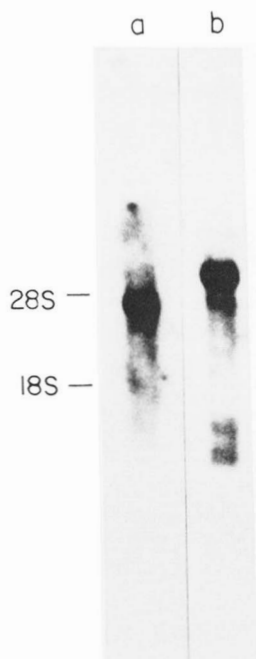


FIG. 3. Northern blot analysis of ORF1 and ORF2. Two  $\mu\text{g}$  of poly(A)<sup>+</sup> RNA prepared from U118-MG cells were fractionated on a formaldehyde agarose gel and transferred onto a nylon membrane. The blot was hybridized to the <sup>32</sup>P-labeled *EcoRI-NotI* 1.2-kb DNA fragment of TM22 (a). Following the removal of this probe the blot was hybridized again to the <sup>32</sup>P-labeled *BstXI-NotI* 1-kb DNA fragment of TM22 (b).

but is not a member of this family or of any of the other known cAMP PDE families.

**Deletion Analysis of HCP1**—To improve the production of HCP1 and to enable our biochemical analysis, we constructed a new expression vector, L22M1. In this vector the first ATG codon was fused to an epitope derived from the influenza virus hemagglutinin transcribed from the strong yeast promoter, ADH1 (30). L22M1 drastically improved the suppression of *pde1<sup>-</sup>pde2<sup>-</sup>* heat shock phenotype (Fig. 5). This improvement may be due, in part, to the removal of the highly GC rich area upstream of the first ATG that might impede transcription and translation. Three additional NH<sub>2</sub>-terminal deletions of HCP1 were generated by sequential deletion of sequences from the first ATG codon to residue 81 (L22M2), 163 (L22M3), and 207 (L22M4). While L22M2 and L22M3 were each capable of efficient suppression of *pde1<sup>-</sup>pde2<sup>-</sup>* defects, the largest deletion mutant, L22M4, failed to do so (Fig. 5). All 10 independent clones of L22M4 that were tested failed to suppress the heat shock sensitivity of 10DAB. Western blot analysis indicated that equivalent amounts of epitope-tagged peptides were produced from all four expression plasmids (L22M1, 63 kDa; L22M2, 50 kDa; L22M3, 43 kDa; L22M4, 39 kDa). Thus, this functional deletion analysis defined the NH<sub>2</sub>-terminal border of the minimal fragment of HCP1 required for cAMP hydrolysis to reside between amino acids 163–207. Interestingly, this border coincides with the NH<sub>2</sub>-terminal border of the conserved domain of cAMP PDEs detailed above (Fig. 4).

**Biochemical Analysis of HCP1**—Substrate and inhibitor kinetic analyses were conducted using crude homogenates from 10DAB cells overexpressing HCP1. The  $K_m$  deduced from the Lineweaver-Burke plots was 0.2  $\mu\text{M}$  cAMP, and the calculated  $V_{max}$  was 0.025 nmol/min · mg total protein (Fig. 6). No cGMP PDE activity was detectable in the overexpressing cells, and no cAMP PDE activity was detected in extracts of

cells carrying an expression vector without an insert. Thus, HCP1 appears to be a cAMP-specific PDE with a very high affinity for cAMP as a substrate. These results suggest that, kinetically, HCP1 has some resemblance to the cGMP-inhibited PDE family in that it has a similar low  $K_m$  for cAMP and that HCP1 also resembles the cAMP-specific PDE family in that it is specific for cAMP.

To determine whether HCP1 is pharmacologically related to the cAMP-specific or the cGMP-inhibited PDE families, we tested whether its PDE activity was sensitive to competitive inhibitors selective to these PDE families (Fig. 7). These compounds are thought to inhibit cAMP hydrolysis by interacting at the catalytic site (31). As expected, cAMP was a potent inhibitor with an  $\text{IC}_{50}$  of 0.2  $\mu\text{M}$  (Fig. 7A). Unlike the cGMP-inhibited PDEs, the PDE activity of HCP1 was virtually unaffected by cGMP. In addition, the cAMP PDE activity of HCP1 was not significantly affected by two specific inhibitors of the cGMP-inhibited PDEs, amrinone and milrinone (Fig. 7B). Although a 50% inhibition of HCP1 was observed in the presence of 60  $\mu\text{M}$  milrinone, an even stronger inhibition of TM72 was observed at these high concentrations of milrinone. TM72 is a high affinity dunce-like cAMP-specific PDE that has been isolated in this screen, and, as a member of this PDE family, is not expected to be particularly sensitive to milrinone. A partially purified bovine lung cGMP-inhibited PDE was, however, sensitive to milrinone with an  $\text{IC}_{50}$  of 1  $\mu\text{M}$ , indicating that the drug was effective during experimental manipulations (data not shown). Thus, it appears that the cAMP activity of HCP1 is not especially sensitive to the known inhibitors of the cGMP-inhibited PDEs.

The cAMP activity of HCP1 was not affected by two potent inhibitors of dunce-like cAMP-specific PDEs, R020-1724 and rolipram (Fig. 7C). TM72, a new member of this dunce-related PDE family, was sensitive to these drugs. Thus, HCP1 appears to be pharmacologically distinct from the dunce-like cAMP-specific PDEs.

**Expression of HCP1 mRNA in Human Tissues**—The abundance of HCP1 mRNA in human tissues was determined on Northern blots probed with the 1.2-kb *NotI-EcoRI* DNA fragment encompassing residues 1–399 of HCP1 (Fig. 8). A 3.8-kb HCP1 mRNA was abundant in skeletal muscle and detectable in kidney and heart. An additional 4.0-kb HCP1 mRNA band was detectable in the brain, kidney, and pancreas. The significance of the two HCP1 transcripts is not known. An additional Northern blot with mRNA samples derived from different individuals had a similar HCP1 mRNA distribution in the heart and skeletal muscle, but its abundance in the brain, kidney, and pancreas was greatly reduced. These blots were subsequently hybridized to an  $\alpha$ -tubulin cDNA probe as a control for RNA concentrations. These results indicate that HCP1 encodes a novel cAMP PDE that is expressed more abundantly in skeletal muscle than in the other tissues we examined.

## DISCUSSION

We have cloned a human cDNA encoding a novel cAMP PDE, HCP1, that is structurally, biochemically, and pharmacologically distinct from known cAMP PDEs. HCP1 is a cAMP PDE with a very high affinity for cAMP ( $K_m = 0.2 \mu\text{M}$ ), a property used to derive its name, high affinity cAMP-specific PDE. Although the sequence of HCP1 is related to those of the Ca<sup>2+</sup>/calmodulin-dependent, the cGMP-stimulated, and the cAMP-specific dunce-like families of cAMP PDEs, the homologies are not as close as those shared between family members, and thus HCP1 is not a member of these

HCP1, a High Affinity cAMP-specific PDE

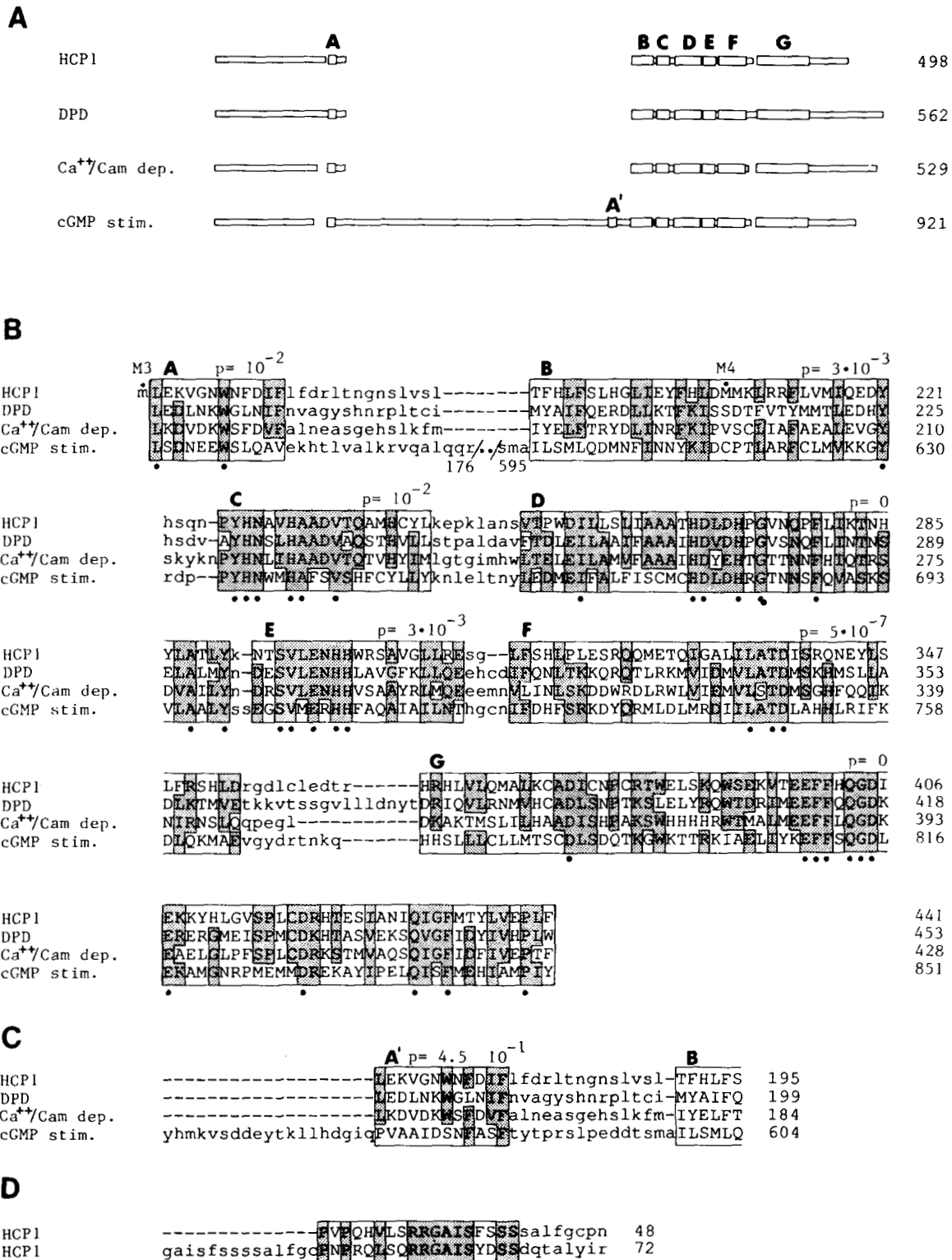


**FIG. 4. Alignment of the amino acid sequences of the HCP1, DPD, Ca<sup>2+</sup>/calmodulin-dependent and cGMP-stimulated PDEs.** The alignment was obtained by the MACAW program (29). *A*, a schematic representation of the alignment of the cyclic nucleotide PDEs. Blocks of homology are boxed and marked A-G. Gaps mark the gaps introduced to maximize homology. *B*, amino acid sequences that constitute homology blocks A-G. Blocks of homology are boxed and capitalized. The probabilities of chance occurrence associated with each block were derived by the MACAW program and are indicated above the blocks. A probability of zero is indicated when the probability of chance occurrence is less than 10<sup>-100</sup>. Dashes indicate gaps introduced to maximize the homology. Coordinates on the right indicate amino acid positions. The location of the NH<sub>2</sub>-terminal border of the peptides expressed from L22M3 (M3) and L22M4 (M4) are depicted above these residues. Residues that are similar among at least three of the four PDEs presented are shaded. Fully conserved residues are under marked with an asterisk (\*). The grouping of similar amino acids are: (V,L,I), (K,R), (E,D), (Q,N), and (S,T). *C*, amino acid sequences that constitute homology block A'. Sequences in this block are identical to those of homology block A except those of the cGMP-stimulated PDE which are located close to homology block B. *D*, a repeat sequence of HCP1. The boxed sequence depicts an 18-residue repeat sequence found by a double-diagonal analysis.

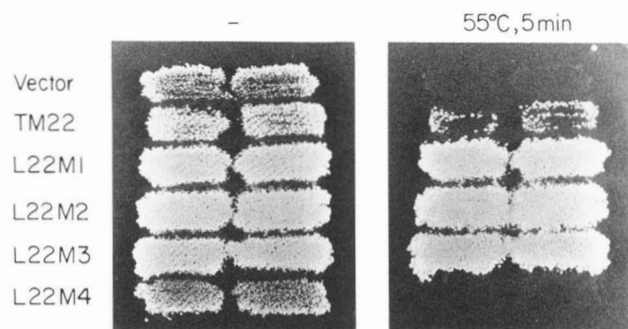


**FIG. 5. Deletion analysis of HCP1.** 10DAB cells were transformed with AD54 (*vector*), with TM22 and with four deletion mutants of HCP1 named L22M1–4. Two independent transformants were patched onto SC-leucine plates, grown at 30 °C for 3 days, and then replica plated onto a control plate and onto an experimental plate that was subjected to a 5-min heat shock treatment at 55 °C. Plates were photographed following a 24-h recovery period at 30 °C.

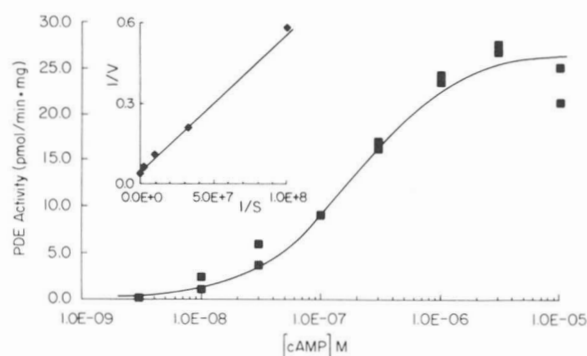


**FIG. 6. Kinetic analysis of HCP1.** cAMP PDE assays were performed on all extracts as described under “Experimental Procedures.” cAMP concentrations ranged from  $3 \cdot 10^{-9}$  to  $10^{-5}$  M. Each data point shown is a measurement of the initial rate of hydrolysis at a suitable enzyme dilution. The *inset* on the upper left corner of the graph depicts the double-reciprocal Lineweaver-Burke plot derived from the kinetics curve.

families. Recently, the sequence of the cGMP-inhibited PDE has been published and HCP1 is not more closely related to this PDE family than to others (32). The kinetic and pharmacological data also suggest that HCP1 represents a member of a new family of cyclic nucleotide PDEs. With respect to substrate specificity, HCP1 most closely resembles the cAMP-specific PDE family (3). However, the apparent affinity for substrate is substantially higher than for any other cAMP-specific PDE, and the enzyme is not inhibited by either rolipram or RO20-1724, potent inhibitors of all known members of this family. The affinity for cAMP is most similar to that of the cGMP-inhibited PDEs, but it is not selectively inhibited by either cGMP or milrinone, a drug that inhibits all the known members of this family. Thus, the HCP1 cAMP PDE is structurally, kinetically and pharmacologically distinct from the currently known high affinity cAMP PDEs. It is possible, of course, that since the 5' end of the HCP1 clone may be truncated that both the substrate and inhibitor specificity could be altered compared to the native enzyme. However, it seems rather unlikely that truncation would increase the apparent affinity for cAMP but decrease the affinity for the drugs and for cGMP. Since the sequence indicates that HCP1 is a separate and highly distinct gene product, it seems more likely that the kinetics reflect intrinsic differences in the properties of the enzyme. HCP1 therefore appears to be a representative of a previously unknown cAMP PDE family, which we now designate as family VII.

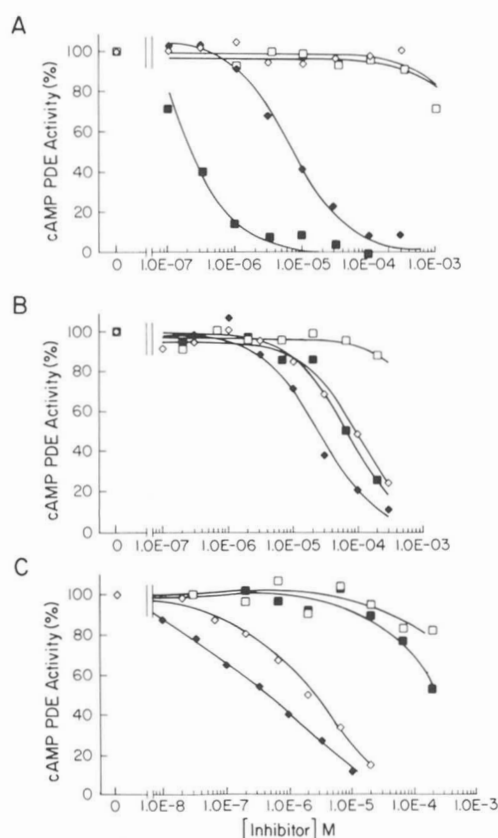


**FIG. 7. Effects of various inhibitors on the cAMP PDE activity of HCP1 and of TM72.** cAMP PDE assays were performed on cell extracts as described under “Experimental Procedures.” Samples included  $3 \cdot 10^{-8}$  M [ $^3$ H]cAMP and the indicated concentrations of inhibitor. *A*, cAMP and cGMP. The indicated concentrations of unlabeled cAMP ( $\blacklozenge$ ,  $\blacksquare$ ) or cGMP ( $\diamond$ ,  $\square$ ) were added to assays. *B*, milrinone and amrinone. The indicated concentrations of milrinone ( $\blacklozenge$ ,  $\blacksquare$ ) or amrinone ( $\diamond$ ,  $\square$ ) were added to the assays. *C*, rolipram and RO20-1724. The indicated concentrations of rolipram ( $\blacklozenge$ ,  $\blacksquare$ ) or RO20-1724 ( $\diamond$ ,  $\square$ ) were added to the assays. *Squares* are extracts harboring HCP1, and *diamonds* are extracts harboring TM72.

Expression of HCP1 was studied by Northern blot analysis of poly(A)<sup>+</sup> RNAs obtained from various human tissues. Two different sized mRNAs were found, 3.8 and 4.0 kb. We do not know if these arise from differential splicing or termination, or if they even arise from the same locus. We have been hampered in these studies by our inability to isolate full-length cDNAs. Low levels of mRNAs were detected in a variety of tissues, including brain and heart. Consistent with this, cDNAs for HCP1 were isolated from cDNA libraries derived from these tissues. We have found high levels of expression of HCP1 transcripts in human skeletal muscle. Very little is known about the expression of cAMP PDEs in skeletal muscle, and this would seem to be the tissue in which to undertake further studies of this cAMP PDE isoform.

The alignment of the HCP1 sequence with those of cAMP PDEs of different families reveals homology to the conserved COOH-terminal catalytic domain of cAMP PDEs. The NH<sub>2</sub>-terminal border of this domain, as defined by the MACAW program, extends 40 residues upstream of the previously delineated border. Our NH<sub>2</sub>-terminal deletion analysis of HCP1 indicated that the minimal fragment required for cAMP hydrolysis encompasses this expanded domain of homology. A peptide lacking this NH<sub>2</sub>-terminal region, and containing the previously delineated conserved domain almost in its entirety, is not catalytically active. These results are in agreement with previous studies of proteolytic fragments of

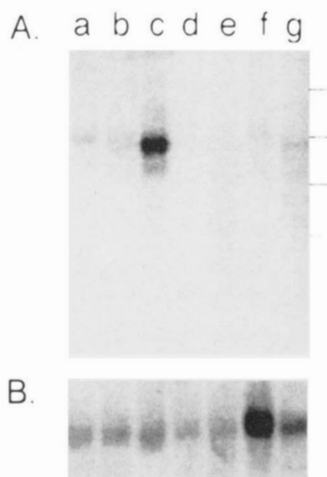


FIG. 8. Tissue distribution of HCP1 mRNA. Two  $\mu\text{g}$  of poly(A)<sup>+</sup> RNA prepared from human pancreas (a), kidney (b), skeletal muscle (c), liver (d), lung (e), brain (f), and heart (g) were fractionated on a denaturing formaldehyde agarose gel and transferred onto a nylon membrane. The blot was hybridized to the <sup>32</sup>P-labeled *NotI*-*EcoRI* 1.2-kb DNA fragment of TM22 (A) and to the <sup>32</sup>P-labeled  $\alpha$ -tubulin cDNA (B). Blots were washed under stringent conditions for 20 min at 65 °C in 0.1  $\times$  SSC. Molecular weight RNA markers are 9.5, 7.5, 4.4, 2.4 and 1.35 kb long, and their migration on the gel is depicted on the right hand side of panel A.

the cGMP-stimulated and the Ca<sup>2+</sup>/calmodulin-dependent PDEs that assigned a catalytic role to a 36-kDa fragment encompassing this conserved domain (24–28). The NH<sub>2</sub>-terminal border of the minimal active fragment of HCP1 is located 17–18 residues downstream of the NH<sub>2</sub> termini of the 36-kDa proteolytic fragments. The catalytically active 36-kDa fragment of the cGMP-stimulated PDE contained homology block A' as detailed in Fig. 4C, and not homology block A which was found by the MACAW program. The role of homology blocks A and A' in catalysis remains to be determined.

We have established a highly sensitive screen for the isolation of cAMP PDEs based on their ability to suppress defects in yeast lacking endogenous cAMP PDEs. We have previously isolated yeast and mammalian cAMP PDEs in the *RAS2<sup>val19</sup>* strain that, like the *pde1<sup>-</sup>pde2<sup>-</sup>* strain, contains elevated intracellular cAMP. Comparisons of the frequency of isolation of one of the cAMP-specific PDEs (JC44) from the library employed in this study indicated that the PDE-deficient yeast strain (10DAB) is almost a hundred-fold more sensitive than the *RAS2<sup>val19</sup>* strain (70/10<sup>5</sup> in *pde1<sup>-</sup>pde2<sup>-</sup>* versus 4/5 · 10<sup>5</sup> in *RAS2<sup>val19</sup>*) for the detection of PDEs.

cDNAs encoding the three different PDEs isolated in this screen failed to suppress the heat shock-sensitive phenotype of *RAS2<sup>val19</sup>*. This seems at first a surprising result since two mammalian cAMP-specific PDEs, rat DPD and human JC44, are capable of suppressing *RAS2<sup>val19</sup>*, and since the intracellular levels of cAMP in *RAS2<sup>val19</sup>* cells are actually lower than those of *pde1<sup>-</sup>pde2<sup>-</sup>* cells (33). This apparent paradox can be understood only in the context of the function of RAS in *S. cerevisiae*. The cAMP PDE activity of these three new human cAMP PDEs are weaker than those of DPD and JC44 when assayed in *pde1<sup>-</sup>pde2<sup>-</sup>* cells (see "Results"). Poor cAMP PDE activity may account for the inability of the newly isolated PDEs to suppress *RAS2<sup>val19</sup>*. RAS appears to control not only the cAMP pathway in *S. cerevisiae* but an additional signaling pathway as well (34). Thus, the heat shock-sensitive pheno-

type of *RAS2<sup>val19</sup>* cells may depend on more than their elevated cAMP content, and therefore may be refractory to the effects of weak cAMP PDEs.

The isolation of cAMP PDEs by complementation of defects in yeast as described in this study has yielded a member of a new cAMP PDE family. The complete sequence of this PDE, the existence of additional members of this family, their distribution, and physiological roles remain to be determined. Additional functional screens in this yeast system may yield additional previously undiscovered PDEs.

**Acknowledgments**—We thank Dr. Paul Feldman, Glaxo Research Institute, Inc., for supplying the rolipram used in this study and the Sterling Drug Company, Inc. for supplying milrinone, Sonja Kalbfleisch and Kim McCaw, ICOS Corporation, for excellent technical assistance, and P. Bird for her help in preparing this manuscript.

#### REFERENCES

- Beavo, J. (1988) in *Advances in Second Messenger and Phosphoprotein Research* (Greengard, P., and Robinson, G. A., eds.) Vol. 22, Raven Press, New York
- Beavo, J., and Houslay, M. D. (eds) (1990) *Cyclic Nucleotide Phosphodiesterases: Structure, Regulation and Drug Action*, Vol. 2, John Wiley and Sons, Ltd., Chichester
- Bentley, J. K., and Beavo, J. A. (1992) *Curr. Opin. Cell Biol.* **4**, 233–240
- Novack, J., Charbonneau, H., Bentley, J., Walsh, K., and Beavo, J. (1991) *Biochemistry* **30**, 7940–7947
- Londesborough, J., and Suoranta, K. (1983) *J. Biol. Chem.* **258**, 2966–2972
- Nikawa, J., Sass, P., and Wigler, M. (1987) *Mol. Cell. Biol.* **7**, 3629–3636
- Sass, P., Field, J., Nikawa, J., Toda, T., and Wigler, M. (1986) *Proc. Natl. Acad. Sci. U. S. A.* **83**, 9303–9307
- Suoranta, K., and Londesborough, J. (1984) *J. Biol. Chem.* **259**, 6964–6971
- Toda, T., Uno, I., Ishikawa, T., Powers, S., Kataoka, T., Broek, D., Cameron, S., Broach, J., Matsumoto, K., and Wigler, M. (1985) *Cell* **40**, 27–36
- Kataoka, T., Powers, S., Cameron, S., Fasano, O., Goldfarb, M., Broach, J., and Wigler, M. (1985) *Cell* **40**, 19–26
- Marshall, M., Gibbs, J., Scolnick, E., and Sigal, I. (1987) *Mol. Cell Biol.* **7**, 2309–2315
- Colicelli, J., Birchmeier, C., Michaeli, T., O'Neill, K., Riggs, M., and Wigler, M. (1989) *Proc. Natl. Acad. Sci. U. S. A.* **86**, 3599–3603
- Colicelli, J., Nicolette, C., Birchmeier, C., Rodgers, L., Riggs, M., and Wigler, M. (1991) *Proc. Natl. Acad. Sci. U. S. A.* **88**, 2913–2917
- Biggin, M. D., Gibson, T. J., and Hong, G. F. (1983) *Proc. Natl. Acad. Sci. U. S. A.* **80**, 3963–3965
- Sanger, F., Nicklen, S., and Coulson, A. R. (1977) *Proc. Natl. Acad. Sci. U. S. A.* **74**, 5463–5467
- Maniatis, T., Fritsch, E., and Sambrook, J. (1982) in *Molecular Cloning, a Laboratory Manual*, Cold Spring Harbor Laboratory, Cold Spring Harbor, NY
- Davis, C., and Daly, J. (1979) *J. Cyclic Nucleotide Res.* **5**, 65–74
- Martins, T., Mummy, M., and Beavo, J. (1982) *J. Biol. Chem.* **255**, 1973–1979
- Livi, G., Kmetz, P., McHale, M., Cieslinski, L., Sathe, G., Taylor, D., Davis, R., Torphy, T., and Balcarek, M. (1990) *Mol. Cell Biol.* **10**, 2678–2686
- Davis, R., Takayasu, H., Eberwine, M., and Myres, J. (1989) *Proc. Natl. Acad. Sci. U. S. A.* **86**, 3604–3608
- Swinnen, J., Joseph, D., and Conti, M. (1989) *Proc. Natl. Acad. Sci. U. S. A.* **86**, 5325–5329
- Proudfoot, N. (1991) *Cell* **64**, 671–674
- Sonnenburg, W., Mullaney, P., and Beavo, J. (1991) **266**, 17655–17661
- Krinks, M. H., Haiech, J., Rhoads, A., and Klee, C. B. (1984) *Adv. Cyclic Nucleotide Res.* **16**, 31–47
- Kincaid, R. L., Stith-Coleman, I. E., and Vaughan, M. (1985) *J. Biol. Chem.* **260**, 9009–9015
- Charbonneau, H., Novack, J. P., MacFarland, R. T., Walsh, K. A., and Beavo, J. A. (1987) in *Calcium-Binding Proteins in Health and Disease* (Norman, A. W., Vanaman, T. C., and Means, A. R., eds) pp. 505–517, Academic Press, Orlando, FL
- Stroop, S. D., Charbonneau, H., and Beavo, J. A. (1989) *J. Biol. Chem.* **264**, 13718–13725
- Charbonneau, H. (1990) in *Cyclic Nucleotide Phosphodiesterases: Structure, Regulation and Drug Action* (Beavo, J., and Houslay, M. D. eds) Vol. 2, pp. 267–296, John Wiley and Sons, Ltd., Chichester
- Schuler, G., Altschul, S., and Lipman, D. (1991) *Proteins Struct. Funct. Genet.* **9**, 180–190
- Field, J., Nikawa, J., Broek, D., MacDonald, B., Rodgers, L., Wilson, I., Lerner, R., and Wigler, M. (1988) *Mol. Cell Biol.* **8**, 2159–2165
- Weishaar, R. E., Cain, M. H., and Bristol, J. A. (1985) *J. Med. Chem.* **28**, 537–545
- Meacci, E., Taira, M., Moos, M., Jr., Smith, C., Movsesian, M., Degerman, E., Belfrage, P., and Manganiello, V. (1992) *Proc. Natl. Acad. Sci. U. S. A.* **89**, 3721–3725
- Nikawa, J., Cameron, S., Toda, T., Ferguson, K., and Wigler, M. (1987) *Genes & Dev.* **1**, 931–937
- Toda, T., Broek, D., Field, J., Michaeli, T., Cameron, S., Nikawa, J., Sass, P., Birchmeier, C., Powers, S., and Wigler, M. (1987) *Oncogene and Cancer* (Aaronson, S. A., et al., eds) pp. 253–260, Japan Scientific Society Press, Tokyo